

Peer reviewed:

Yes, submitted to Mathematics and Mechanics of Solids

Title:

A monolithic phase-field model of a fluid-driven fracture in a nonlinear poroelastic medium

Author:

C.J. van Duijn^{1,2}, Andro Mikelic³, and Thomas Wick⁴

1. Department of Earth Sciences, Utrecht University, P.O. Box 80021, 3508TA Utrecht, The Netherlands
2. Department of Mechanical Engineering, Eindhoven University of Technology, P.O. Box 513, 5600 MB Eindhoven, The Netherlands
3. Univ Lyon, Universite Claude Bernard Lyon 1, CNRS UMR 5208, Institut Camille Jordan, 43 blvd. du 11 novembre 1918, F-69622 Villeurbanne cedex, France
4. Institut für Angewandte Mathematik, Leibniz Universität Hannover, Welfengarten 1, 30167 Hannover, Germany

Publication date:

4-2018

Copyright information:

Copyright and moral rights for the publications made accessible in the public portal are retained by the authors and/or other copyright owners and it is a condition of accessing publications that users recognise and abide by the legal requirements associated with these rights. Users may download and print one copy of any publication from the public portal for the purpose of private study or research. You may not further distribute the material or use it for any profit-making activity or commercial gain. You may freely distribute the URL identifying the publication in the public portal.

A monolithic phase-field model of a fluid-driven fracture in a nonlinear poroelastic medium

submitted to **Mathematics and Mechanics of Solids**, ISDMM 2017 Special Issue
XX(X):1–15
© The Author(s) 2018
Reprints and permission:
sagepub.co.uk/journalsPermissions.nav
DOI: 10.1177/ToBeAssigned
www.sagepub.com/



C.J. van Duijn¹, Andro Mikelić² and Thomas Wick³

Abstract

In this paper we present a full phase field model for a fluid-driven fracture in a *nonlinear* poroelastic medium. The poroelastic medium contains an incompressible elastic skeleton and the pores are filled with an incompressible viscous fluid. The regime is quasi-static and the permeability depends on the porosity, which is itself a function of the skeleton volume strain. In our previous work (see²⁵ [A. Mikelić, M. F. Wheeler, T. Wick: Phase-field modeling of a fluid-driven fracture in a poroelastic medium, Computational Geosciences, Vol. 19(2015), no. 6, 1171-1195]) we considered a fully coupled system where the pressure is determined simultaneously with the displacement and the phase field, for the linearized quasi-static Biot equations. For the new model, we establish existence of a solution to the incremental problem through convergence of a finite dimensional approximation. Furthermore, we construct the corresponding Lyapunov functional that is linked to the free energy. Computational results are provided that demonstrate the effectiveness of this approach in treating fluid-driven fracture propagation. Specifically, our numerical findings confirm differences with test cases using the linear Biot equations.

Keywords

Hydraulic fracturing, Phase field, Nonlinear poroelasticity

Introduction

In this paper, we further develop phase-field models for fluid-driven fractures in porous media. To the best of our knowledge, existing models use the linear Biot equations, e.g.,^{6,15,18,19,21,22,24}. Here we extend previous work²⁵, by considering a phase-field model that uses nonlinear Biot equations in which the permeability depends on the porosity (and thus on the displacements). We formulate a fully coupled system in which the displacement and phase-field variables (\mathbf{u}, φ) and the pressure p are treated simultaneously. This allows us to introduce a free energy functional.

In contrast to²³⁻²⁴, the phase field approach presented here does not require high regularity of the variable φ . Hence it can be used in a more general setting.

Mathematical model: pressure equations and poroelasticity

In this section, we present the equations and additional conditions that describe the problem of a fluid driven crack surrounded by poroelastic material. The primary unknowns of the problem are the fluid pressure p_R in the porous medium, its displacement \mathbf{u} and the fluid pressure p_F in the crack. An equation for p_R results from the mass-balances of the fluid and the solid in the porous domain. The displacement \mathbf{u} and the pressure p_R are related through the classical quasi-static Biot equations. The pressure p_F in the crack results from a lubrication approximation since cracks or fractures generally are "penny" shaped: they extend in two directions and are thin in the orthogonal cross direction.

We treat in some detail the derivation of the mass balance equation in the poroelastic medium, at which we follow^{3, 20} and²⁷. At various stages of the derivation, the equations are simplified. Throughout, however, we consider the permeability to be a function of the porosity. This dependence results in a nonlinear coupling of the equations.

We start with some geometrical considerations.

Geometry

Let \mathcal{C} denote any open set homeomorphic to an ellipsoid in \mathbb{R}^3 (a crack set). Its boundary $\partial\mathcal{C} = \Gamma$ is a closed surface. In most applications \mathcal{C} is a curved 3D domain, with one dimension significantly smaller than the other dominant two. An example is a penny shaped crack.

The crack set \mathcal{C} is surrounded by the poroelastic domain $\Omega = B \setminus \bar{\mathcal{C}}$, where $B = (0, L)^3 \supset \supset \mathcal{C}$.

¹ Darcy Center, Eindhoven University of Technology, Department of Mechanical Engineering and Utrecht University, Department of Earth Sciences, The Netherlands

² Univ Lyon, Université Claude Bernard Lyon 1, CNRS UMR 5208, Institut Camille Jordan, 43 blvd. du 11 novembre 1918, F-69622 Villeurbanne cedex, France

³ Institut für Angewandte Mathematik, Leibniz Universität Hannover, Welfengarten 1, 30167 Hannover, Germany

Corresponding author:

Andro Mikelić,
Univ Lyon, Université Claude Bernard Lyon 1, CNRS UMR 5208, Institut Camille Jordan, 43 blvd. du 11 novembre 1918, F-69622 Villeurbanne cedex, France

Email: mikelic@univ-lyon1.fr

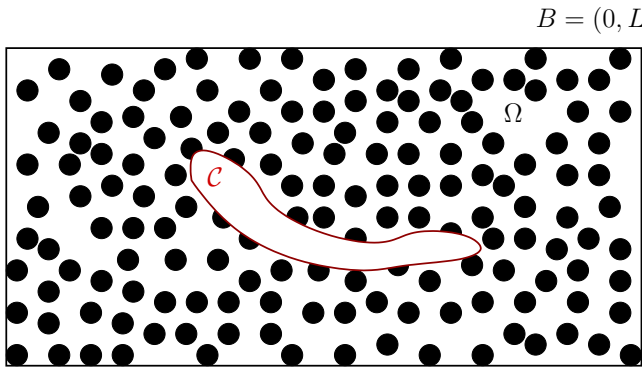


Figure 1. A crack C embedded in a porous medium. Here, the dimensions of the crack are assumed to be much larger than the pore scale size (black dots) of the porous medium.

In much of the fracture propagation literature, see e. g. ¹ and ¹²⁾, the cracks are treated as lower dimensional manifolds in which lubrication theory is applied to describe the fluid flow (see ¹⁴⁾.

However, the interaction of the poroelastic biphasic medium with the fluid flow is not well understood. Therefore, we consider C as a thin 3D object to which we apply the lubrication approach. As a result, we obtain an expression for the permeability in the crack. The model is completed by introducing a Griffith-type surface energy, which we use in a regularized form.

The boundary of $B = (0, L)^3$ is denoted by ∂B , which is divided into open 2D surfaces $\partial_D B$ and $\partial_N B$, with smooth boundaries, in the way that $\partial B = \overline{\partial_D B} \cup \overline{\partial_N B}$. On $\partial_D B$ Dirichlet boundary conditions are imposed and on $\partial_N B$ Neumann conditions, respectively. We assume that $\text{meas}(\partial_D B) > 0$. On $\partial_D B$ the displacement and fluid flux is prescribed, on $\partial_N B$ a load and the fluid pressure. The boundary conditions are given smooth functions.

Porous Medium

We assume that the porous domain Ω , having porosity n , is fully saturated with a fluid of density ρ_R . Let \mathbf{v}_R denote the average fluid velocity in the pores. Then $\mathbf{q}_R = n\mathbf{v}_R$ is the specific discharge of the fluid and $\mathbf{j}_R = \rho_R \mathbf{q}_R = n\rho_R \mathbf{v}_R$ its mass flow.

In the Darcy law, the velocity is considered relative to the movement of the skeleton. To this end we write

$$\mathbf{v}_R = \mathbf{v}_{R,r} + \mathbf{v}_s, \quad (1)$$

where $\mathbf{v}_{R,r}$ is the fluid velocity relative to the velocity \mathbf{v}_s of the skeleton.

Remark 1. If $\mathbf{x} = \mathbf{x}(\xi, t)$ denotes the location of a solid particle starting at $\mathbf{x}(\xi, 0) = \xi$, one has $\mathbf{v}_s = \partial_t \mathbf{x}|_{\xi}$.

With (1) the specific discharge reads

$$\mathbf{q}_R = \mathbf{q}_{RD} + n\mathbf{v}_s, \quad (2)$$

where \mathbf{q}_{RD} is the Darcy discharge given by

$$\mathbf{q}_{RD} = \frac{\mathbb{K}_R k_R(n)}{\eta_R} (\rho_R \mathbf{g} - \nabla p_R). \quad (3)$$

Here \mathbb{K} is the absolute permeability tensor (a positive definite second order tensor) and $k_R(n)$ is a function describing the

porosity dependence of the permeability. Furthermore, η_R is the fluid viscosity, p_R the fluid pressure and \mathbf{g} the gravity vector. The function $k_R : [0, 1] \rightarrow [0, +\infty)$ is smooth and strictly increasing. If ℓ is the characteristic pore size, a well-known example is the Kozeny-Carman relation (see e.g. ³⁾)

$$k_R(n) = k_{ref} \frac{n^3}{(1-n)^2}, \quad k_{ref} > 0, \quad (4)$$

where k_{ref} is proportional to ℓ^2 . Another example is $k_R(n) = k_{ref} n^{5.1}$, valid for an array of cylinders (see ¹⁷⁾. The range of validity of expression (4) is $0.35 \leq n \leq 0.67$. To have it defined on $[0, 1]$ we propose the extension (see also ⁷⁾):

$$k_R(n) = \begin{cases} k_{ref} \frac{n^3}{(1-n)^2}, & \text{for } 0 < n_* < n < n^* < 1, \\ k_{ref} \frac{(n^*)^3}{(1-n^*)^2}, & \text{for } n \geq n^*, \\ k_{ref} \frac{n_*^3}{(1-n_*)^2}, & \text{for } n \leq n_*. \end{cases} \quad (5)$$

Corresponding to (1) we have the mass flux

$$\mathbf{j}_R = \mathbf{j}_{RD} + n\rho_R \mathbf{v}_s. \quad (6)$$

Next, we consider the mass balances. For the porous medium fluid we have

$$\partial_t(n\rho_R) + \text{div } \mathbf{j}_R = Q, \quad (7)$$

where Q denotes a source/sink term, and for the solid

$$\partial_t((1-n)\rho_s) + \text{div } ((1-n)\rho_s \mathbf{v}_s) = 0. \quad (8)$$

In (8), ρ_s is the density of the skeleton material. Using (6) in (7) gives

$$\partial_t(n\rho_R) + \text{div } (n\rho_R \mathbf{v}_s) = -\text{div } \mathbf{j}_{RD} + Q$$

or

$$\partial_t(n\rho_R) + \mathbf{v}_s \cdot \nabla(n\rho_R) + n\rho_R \text{div } \mathbf{v}_s = -\text{div } \mathbf{j}_{RD} + Q. \quad (9)$$

Introducing the material derivative

$$\frac{D}{Dt} = \partial_t + \mathbf{v}_s \cdot \nabla,$$

we obtain the Lagrangian form of (7) and (8)

$$\frac{D(n\rho_R)}{Dt} + n\rho_R \text{div } \mathbf{v}_s = -\text{div } \mathbf{j}_{RD} + Q \quad (10)$$

and

$$\frac{D((1-n)\rho_s)}{Dt} + (1-n)\rho_s \text{div } \mathbf{v}_s = 0. \quad (11)$$

From (11) we deduce

$$\frac{Dn}{Dt} = \frac{(1-n)}{\rho_s} \frac{D\rho_s}{Dt} + (1-n) \text{div } \mathbf{v}_s.$$

Substituting this into (10) gives

$$n \frac{D\rho_R}{Dt} + \rho_R \left(\text{div } \mathbf{v}_s + \frac{(1-n)}{\rho_s} \frac{D\rho_s}{Dt} \right) = -\text{div } \mathbf{j}_{RD} + Q. \quad (12)$$

Equations (11) and (12) are the rewritten mass balance equations. They contain, as an a priori unknown, the skeleton deformation velocity \mathbf{v}_s . If \mathbf{u} denotes the displacement of the skeleton, then

$$\mathbf{v}_s = \frac{D\mathbf{u}}{Dt}. \quad (13)$$

To determine \mathbf{u} we introduce the well-known quasi-static Biot equations (see references⁸ and²⁹)

$$-\operatorname{div}(\sigma^{por}) = \rho_b \mathbf{g}, \quad (14)$$

where

$$\sigma^{por} - \sigma_0 = \mathcal{G}e(\mathbf{u}) - \alpha p_R \mathbb{I}. \quad (15)$$

Here σ is a total stress tensor, $\rho_b = n\rho_R + (1-n)\rho_s$ the bulk density of the porous medium, \mathcal{G} the Gassmann tensor (symmetric positive definite rank-4 tensor), $e(\mathbf{u})$ the strain tensor and $\alpha \in (0, 1]$ the Biot coefficient. Further, σ_0 is the reference state of the total stress.

For simplicity, we restrict ourselves to the case of linear elasticity, where the effective stress tensor σ' is given by

$$\sigma' = \mathcal{G}e(\mathbf{u}) = 2\mu e(\mathbf{u}) + \lambda \operatorname{tr}(e(\mathbf{u}))\mathbb{I} = 2\mu e(\mathbf{u}) + \lambda \operatorname{div} \mathbf{u} \mathbb{I},$$

where \mathbb{I} is the identity matrix, $\operatorname{tr}(\cdot)$ the trace operator, and μ and λ are Lamé's parameters. They are linked to Young's modulus E and Poisson's ratio ν_s by

$$\mu = \frac{E}{2(1+\nu_s)} \quad \text{and} \quad \lambda = \frac{E\nu_s}{(1+\nu_s)(1+2\nu_s)}.$$

To close the system (11), (12) and (14)-(15) we need constitutive relations for ρ_R and ρ_s . As in Lewis-Schrefler²⁰ or Rutquist²⁷ we suppose

$$\rho_R = \rho_R(p_R), \quad (16)$$

with $c_R = \frac{d\rho_R}{dp_R} \geq 0$ denoting the fluid compressibility, and

$$\begin{aligned} \frac{\rho_s}{\rho_{s0}} &= 1 + \frac{p_R - p_{R0}}{K_s} - \frac{\operatorname{tr}(\sigma' - \sigma'_0)}{(1-n)3K_s} = \\ &= 1 + \frac{p_R - p_{R0}}{K_s} - \frac{(3\lambda + 2\mu)}{(1-n)3K_s} \operatorname{div} \mathbf{u}, \end{aligned} \quad (17)$$

where K_s is the bulk modulus of the skeleton material and ρ_{s0} and p_{R0} are reference values. Having a finite but large K_s means that the skeleton is weakly compressible. As a consequence, $\rho_s > 0$.

Hence, the system (11), (12) and (14)-(15), together with (16) and (17), yields a coupled system of nonlinear PDE's for the unknowns n , p_R and \mathbf{u} .

The important parameters and unknowns are listed in the Table 1.

In the following, we make a number of simplifications:

A. Let T , L and u_c be characteristic values of time, length and displacement, respectively. Then we have, with u_c/T being the characteristic skeleton velocity,

$$\frac{D}{Dt} = \frac{1}{T} \left(\partial_t + \frac{u_c}{L} \mathbf{v}_s \cdot \nabla \right),$$

Table 1. Summary of unknowns and effective coefficients.

Symbol	Quantity	Unit
\mathbf{u}	Solid displacement	m
p_i	Fluid pressure: i=R(ock), i=F(racture)	Pa
σ^{por}	Total poroelasticity tensor	Pa
$e(\mathbf{u})$	Linearized strain tensor	–
\mathbb{K}_R	Permeability tensor porous domain	Darcy
k_R	Relative permeability: $k_R = k_R(n)$	–
\mathbb{K}_F	Permeability tensor in fracture	Darcy
α	Biot's coefficient	–
η_i	Fluid viscosity: i=R(ock), i=F(racture)	kg/m sec
\mathcal{G}	Gassman rank-4 tensor	Pa
ρ_i	Fluid density: i=R(ock), i=F(racture)	kg/m ³
n	porosity	–

where the term $\partial_t + \frac{u_c}{L} \mathbf{v}_s \cdot \nabla$ on the right hand side is dimensionless. Since we are in the linear elastic regime we have $\frac{u_c}{L} \ll 1$. This allows us to replace $\frac{D}{Dt}$ by ∂_t in equations (11) and (12).

The result is

$$\partial_t((1-n)\rho_s) + (1-n)\rho_s \operatorname{div} \mathbf{v}_s = 0 \quad (18)$$

and

$$n\partial_t \rho_R + \rho_R \left(\operatorname{div} \mathbf{v}_s + \frac{(1-n)}{\rho_s} \partial_t \rho_s \right) = -\operatorname{div} \mathbf{j}_{RD} + Q. \quad (19)$$

Equation (18) can be integrated to give

$$(1-n)\rho_s = (1-n_0)\rho_{s0} e^{-\int_0^t \operatorname{div} \mathbf{v}_s(x,\tau) d\tau}, \quad (20)$$

where $0 < n_0 < 1$ is the porosity at $t = 0$. This equation shows that the porosity has the natural upper bound

$$n < 1.$$

Within the validity of the approximation we may write

$$\operatorname{div} \mathbf{v}_s = \partial_t \operatorname{div} \mathbf{u}. \quad (21)$$

Using this in (20) gives

$$(1-n)\rho_s = (1-n_0)\rho_{s0} e^{-\operatorname{div} \mathbf{u}}. \quad (22)$$

Here we assumed that the displacement $\mathbf{u} = 0$ in the initial reference state. Expressions (17) and (22) allow us to write n in the terms of p_R and $\operatorname{div} \mathbf{u}$. In a linearized sense this gives

$$\begin{aligned} n &= n_0 + (1-n_0) \frac{p_R - p_{R0}}{K_s} \\ &+ (1-n_0) \left(1 - \frac{3\lambda + 2\mu}{(1-n_0)3K_s} \right) \operatorname{div} \mathbf{u}. \end{aligned} \quad (23)$$

Substituting this relation, or the general nonlinear form, into equation (19) yields a nonlinear equation in terms of p_R and $\operatorname{div} \mathbf{u}$.

B. Incompressible grains: $K_s = +\infty$.

Then from (17) we have

$$\rho_s = \rho_{s0} = \text{constant in time}, \quad (24)$$

and from (22)

$$1 - n = (1 - n_0)e^{-\text{div } \mathbf{u}}. \quad (25)$$

Linearizing yields

$$n = n_0 + (1 - n_0) \text{div } \mathbf{u}. \quad (26)$$

Using (24) and (26) in (19) yields the nonlinear pressure equation

$$n c_R \partial_t p_R + \rho_R \text{div } \partial_t \mathbf{u} = -\text{div} \left(\frac{\mathbb{K}_R k_R(n) \rho_R}{\eta_R} (\rho_R \mathbf{g} - \nabla p_R) \right) + Q, \quad (27)$$

where $c_R = c_R(p_R)$, $\rho_R = \rho_R(p_R)$ and n satisfies (25) or (26).

C. Incompressible fluid: ρ_R is constant.

Then $c_R = 0$ and one is left with

$$\text{div } \partial_t \mathbf{u} + \text{div} \left(\frac{\mathbb{K}_R k_R(n) \rho_R}{\eta_R} (\rho_R \mathbf{g} - \nabla p_R) \right) = Q_R. \quad (28)$$

where $Q_R = Q/\rho_R$.

Fracture

The fracture \mathcal{C} , which is surrounded by the poroelastic body Ω , contains fluid only. Since fractures in general have a flat shape (they usually extend in two directions and are flat in the orthogonal cross direction), they are often treated as lower dimensional objects in classical fracture mechanics. In these lower dimensional objects; one then applies a lubrication approximation when fluid is present, as in the case of porous media.

Since it is difficult to couple the lower dimensional fracture equation with the 3D poroelasticity equations, one formulates a 3D Darcy law in the fracture as well. This approach was developed in²⁴. The derivation of the 3D Darcy law uses the lubrication approach in which one keeps the variable in the cross direction. Clearly, the obtained law depends on the choice of the flow condition at the fracture boundary Γ .

If one imposes that away from the tip the fracture boundary moves with the velocity \mathbf{v}_s of the skeleton and that the fracture fluid satisfies a no-slip condition at Γ , then the results from²⁴ apply. Supposing a tangential slip of the fluid flow at Γ , for instance the tip velocity of the crack, would give additional terms in the effective 3D Darcy law.

The method developed in²⁴, which uses ideas from classical lubrication theory (e.g. Hamrock et al¹⁴), yields the following results.

Let $\{x_1, x_2, x_3\}$ form a local orthogonal coordinate system in which we describe the fluid fracture \mathcal{C} . With reference to Figure 2, the width of the fracture is given by

$$w(x_1, x_2, t) = h^{(2)}(x_1, x_2, t) - h^{(1)}(x_1, x_2, t).$$

At Γ and away from tip one has

$$\mathbf{q}_F \cdot \mathbf{n} = \partial_t \mathbf{u} \cdot \mathbf{n}.$$

At $x_3 = h^{(2)}$ this implies to leading order

$$\partial_t u_3 = \partial_t h^{(2)} = q_{F3}.$$

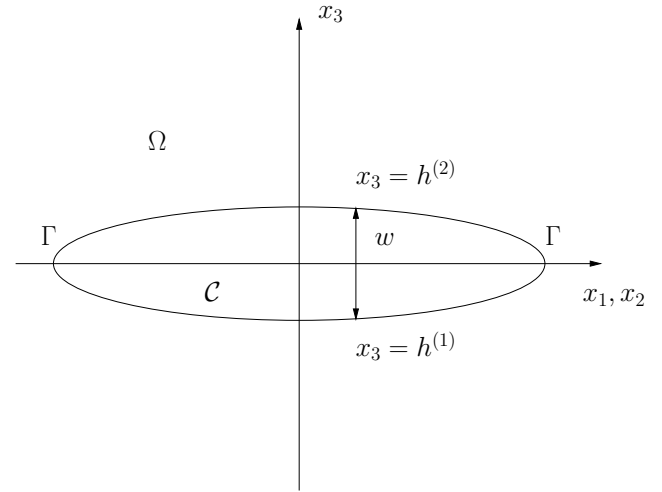


Figure 2. Fracture expressed in the local coordinate system $\{x_1, x_2, x_3\}$

In the fracture \mathcal{C} we have

$$\mathbf{q}_F = \mathbf{q}_{FD} + \mathcal{V} \mathbf{e}_3, \quad (29)$$

where \mathbf{q}_{FD} has the Darcy form

$$\mathbf{q}_{FD} = \frac{\mathbb{K}_F}{\eta_F} (\rho_F \mathbf{g} - \nabla p_F). \quad (30)$$

In (29) \mathbf{q}_F denotes the absolute fluid discharge (or velocity, since the porosity $n = 1$ in the fracture) and $\mathcal{V} \mathbf{e}_3$ the vertical discharge component due to the rate of change of $h^{(1)}$ and $h^{(2)}$. The factor \mathcal{V} is given by

$$\mathcal{V} = \left(1 - \frac{K_e}{K_{abs}}\right) \partial_t h^{(2)} + \frac{K_e}{K_{abs}} \partial_t h^{(1)}, \quad (31)$$

where

$$K_e = K_e(x_3; h^{(1)}, h^{(2)}) = \frac{(h^{(2)} - x_3)^2}{12} (h^{(2)} + 2x_3 - 3h^{(1)}), \quad (32)$$

and

$$K_{abs} = K_{abs}(h^{(1)}, h^{(2)}) = \frac{(h^{(2)} - h^{(1)})^3}{12} = \frac{w^3}{12}. \quad (33)$$

In (30), η_F is the fluid viscosity in the fracture, ρ_F the fluid density and p_F the fluid pressure. Finally, the permeability tensor \mathbb{K}_F is given by

$$\mathbb{K}_F = K_F \mathbb{I}, \quad (34)$$

where

$$K_F = K_F(x_3; h^{(1)}, h^{(2)}) = \frac{1}{2} (h^{(2)} - x_3)(x_3 - h^{(1)}). \quad (35)$$

Note that in flat fractures, the dominant velocity is in the two dimensional (x_1, x_2) -direction.

Thus in this approximation, the fluid in the fractures behaves as if it moves through a porous medium where the permeability is given by (34)-(35) and where the porosity $n = 1$.

Supposing that the fluid in the fracture is incompressible as well, the pressure p_F satisfies the mass conservation equation

$$\operatorname{div} \mathbf{q}_F = \operatorname{div} \left(-\frac{\mathbb{K}_F}{\eta_F} (\nabla p_F - \rho_F \mathbf{g}) + \mathcal{V} \mathbf{e}_3 \right) = Q_F, \quad (36)$$

where Q_F is a source/sink term in the fracture.

Interface Conditions

The composite domain $\mathcal{C} \cup \Gamma \cup \Omega$ can be seen as an effective porous medium with an interface $\Gamma = \Gamma(t)$ (the boundary of the fracture) across which the fluid density and the porosity may be discontinuous: $\rho_R \neq \rho_F$ for certain applications and $n_F = 1 > n$.

Considering the mass balance for the fluid in $\mathcal{C} \cup \Gamma \cup \Omega$

$$\partial_t(n\rho) + \operatorname{div}(\rho \mathbf{q}) = 0,$$

we have the Rankine-Hugoniot condition at Γ

$$\mathbf{v}_\Gamma \cdot \mathbf{n} = \frac{[\rho \mathbf{q} \cdot \mathbf{n}]}{[\rho n]} = \frac{\rho_R \mathbf{q}_R \cdot \mathbf{n} - \rho_F \mathbf{q}_F \cdot \mathbf{n}}{n\rho_R - \rho_F} \Big|_{\Gamma(t)}. \quad (37)$$

Here \mathbf{v}_Γ is the velocity of $\Gamma(t)$ and \mathbf{n} the unit normal to $\Gamma(t)$.

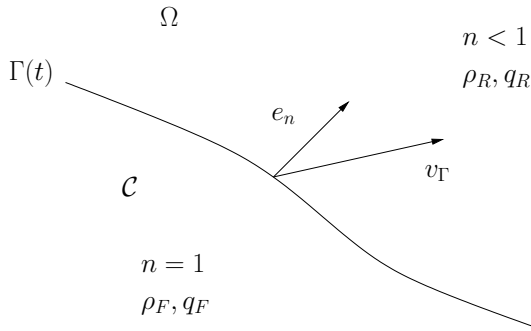


Figure 3. Movement of the fracture boundary $\Gamma(t)$

In expression (37) \mathbf{q} denotes the absolute discharge. At the tip of the fracture the elasticity assumption fails and plastic deformation determines the behavior. In the next section we introduce the phase field approach to deal with this situation. Away from the tip linear elasticity behavior holds and we have for the velocity of the interface

$$\mathbf{v}_\Gamma = \frac{\partial \mathbf{u}}{\partial t} \Big|_\Gamma = \mathbf{v}_s \Big|_\Gamma.$$

Thus at these points of $\Gamma(t)$ where this holds

$$\mathbf{q}_R = \mathbf{q}_{RD} + n \mathbf{v}_\Gamma. \quad (38)$$

Since \mathbf{q}_F satisfies (29) and $\mathcal{V}|_{\{x_3=h^{(i)}\}} = \partial_t h^{(i)}$ for $i = 1, 2$, we have at $\Gamma(t)$

$$\mathbf{q}_F = \mathbf{q}_{FD} + \partial_t h^{(i)} \mathbf{e}_3, \quad i = 1, 2.$$

To the leading order this implies

$$\mathbf{q}_F = \mathbf{q}_{FD} + \mathbf{v}_\Gamma. \quad (39)$$

In (38) and (39), \mathbf{q}_{RD} and \mathbf{q}_{FD} are given by, respectively, (3) and (30). With (38)-(39), the Rankine-Hugoniot condition

(37) reduces to the interface condition

$$\rho_F \mathbf{q}_{FD} \cdot \mathbf{n} = \rho_R \mathbf{q}_{RD} \cdot \mathbf{n} \quad (40)$$

on the moving interface $\Gamma(t)$. This condition is supplemented by pressure continuity

$$p_R = p_F \quad \text{at } \Gamma(t), \quad (41)$$

and normal stress continuity

$$\sigma^{por} \mathbf{n} = -p_F \mathbf{n} \quad \text{at } \Gamma(t). \quad (42)$$

Condition (40) is used in²⁴, Sec 2.3. Condition (41) is a simplification of the pressure interface conditions. More careful modeling by upscaling indicates the presence of an additional term as for instance in the slip law by Beavers and Joseph. We do not dwell on this question here. For a different modeling of the interface fracture/surrounding medium, we refer to¹⁰ and references therein.

Mathematical model: phase field formulation

Since we are primarily interested in a fracture propagating due to pressures induced by water injection, we keep the source/sink terms in the equations, set the reference stress $\sigma_0 = 0$, $\alpha = 1$ and disregard gravity effects. We summarize the resulting equations.

In the poroelastic domain Ω , we have

$$\operatorname{div} \partial_t \mathbf{u} - \operatorname{div} \left(\frac{\mathbb{K} k_R(n)}{\eta_R} \nabla p_R \right) = Q_R, \quad (43)$$

$$-\operatorname{div} \sigma^{por} = 0, \quad \sigma^{por} = \mathcal{G} e(\mathbf{u}) - p_R \mathbb{I}. \quad (44)$$

In the thin fracture \mathcal{C} , we have

$$\operatorname{div} \left(-\frac{\mathbb{K}_F}{\eta_F} \nabla p_F + \mathcal{V} \mathbf{e}_3 \right) = Q_F, \quad (45)$$

where \mathbb{K}_F is given by (34)-(35).

The coupling at the fracture boundary Γ is given by

$$p_R = p_F; \quad \sigma^{por} \mathbf{n} = -p_F \mathbf{n}; \quad (46)$$

$$\rho_{R0} \frac{\mathbb{K} k_R(n)}{\eta_R} \nabla p_R \cdot \mathbf{n} = \rho_{F0} \frac{\mathbb{K}_F}{\eta_F} \nabla p_F \cdot \mathbf{n}. \quad (47)$$

These equations and coupling conditions describe the elastic (i.e. small displacement) behavior of the system. In particular, the movement of the fracture boundary Γ is given by $\frac{\partial \mathbf{u}}{\partial t} \Big|_\Gamma$. Hence only small displacements are allowed.

System (43)-(47) is studied in a weak form which does not involve the fracture boundary $\Gamma(t)$. We set

$$p = \begin{cases} p_R & \text{in } \Omega, \\ p_F & \text{in } \mathcal{C}, \end{cases} \quad (48)$$

and have the following result:

Proposition 2. For a given fracture $\mathcal{C}(t)$, let $\{\mathbf{u}, p\}$ be a smooth solution of (43)-(47), satisfying the boundary conditions

$$-\frac{\mathbb{K} k_R(n)}{\eta_R} \nabla p \cdot \mathbf{n} = v^{inj} \quad \text{and} \quad \mathbf{u} = 0 \quad \text{on } \partial_D B, \quad (49)$$

$$\mathcal{G} e(\mathbf{u}) \mathbf{n} = \tau + p^{bdry} \mathbf{n} \quad \text{and} \quad p = p^{bdry} \quad \text{on } \partial_N B. \quad (50)$$

Then $\{\mathbf{u}, p\}$ satisfies the variational equations

$$\int_{\Omega} \mathcal{G}e(\mathbf{u}) : e(\xi) dx + \int_{\Omega} \nabla p \cdot \xi dx - \int_{\partial_{NB}} (\tau + p^{bdry} \mathbf{n}) \cdot \xi dS = 0, \quad (51)$$

for all $\xi \in V_U = \{\mathbf{z} \in H^1(\Omega)^3 \mid \xi|_{\partial_{DB}} = 0\}$, and

$$\begin{aligned} & \int_{\Omega} \operatorname{div} \left((1 - \frac{\rho_{F0}}{\rho_{R0}}) \partial_t \mathbf{u} \right) \psi dx - \int_{\Omega} \frac{\rho_{F0}}{\rho_{R0}} \partial_t \mathbf{u} \cdot \nabla \psi dx \\ & + \int_{\Omega} \frac{\mathbb{K}k_R(n)}{\eta_R} \nabla p \cdot \nabla \psi dx + \int_{\mathcal{C}} \frac{\rho_{F0}}{\rho_{R0}} \frac{\mathbb{K}_F}{\eta_F} \nabla p \cdot \nabla \psi dx \\ & = \int_{\Omega} Q_R \psi dx + \int_{\mathcal{C}} \frac{\rho_{F0}}{\rho_{R0}} Q_F \psi dx - \int_{\partial_{DB}} v^{inj} \psi dS, \end{aligned} \quad (52)$$

for all $\psi \in V_P = \{\gamma \in H^1(\Omega \cup \Gamma \cup \mathcal{C}) \mid \gamma = 0 \text{ on } \partial_{NB}\}$.

Proof. Equation (51) was derived and used in²³, pages 1375-1376, where it served as basis for the development of the phase field formulation. For this reason, we only discuss briefly the derivation of equation (52).

In the fracture \mathcal{C} , the weak form of equation (45) is

$$\begin{aligned} & \int_{\mathcal{C}} \rho_{F0} \operatorname{div} (\mathcal{V} \mathbf{e}_3) \psi dx - \int_{\mathcal{C}} \rho_{F0} \mathbf{q}_{FD} \cdot \nabla \psi dx + \\ & \int_{\Gamma} \rho_{F0} \mathbf{q}_{FD} \cdot \mathbf{n}_F = \int_{\mathcal{C}} \rho_{F0} Q_F \psi dx, \\ & \forall \psi \in H^1(\Omega \cup \Gamma \cup \mathcal{C}), \psi = 0 \text{ on } \partial_{NB}. \end{aligned} \quad (53)$$

Clearly,

$$\int_{\mathcal{C}} \operatorname{div} (\mathcal{V} \mathbf{e}_3) \psi dx = \int_{\Gamma} \mathcal{V} \mathbf{e}_3 \cdot \mathbf{n}_F \psi dS - \int_{\mathcal{C}} \mathcal{V} \partial_{x_3} \psi dx.$$

Writing $\Gamma = \Gamma_{\{x_3 > 0\}} \cup \Gamma_{\{x_3 \leq 0\}}$, we have

$$\begin{aligned} & \int_{\Gamma} \mathcal{V} \mathbf{e}_3 \cdot \mathbf{n}_F \psi dS = \int_{\Gamma_{\{x_3 > 0\}}} \partial_t h^{(2)} \mathbf{e}_3 \cdot \mathbf{n}_F \psi dS + \\ & \int_{\Gamma_{\{x_3 < 0\}}} \partial_t h^{(1)} \mathbf{e}_3 \cdot \mathbf{n}_F \psi dS \\ & = \int_{\Gamma_{\{x_3 > 0\}}} \partial_t u_3 \mathbf{e}_3 \cdot \mathbf{n}_F \psi dS + \int_{\Gamma_{\{x_3 < 0\}}} \partial_t u_3 \mathbf{e}_3 \cdot \mathbf{n}_F \psi dS. \end{aligned}$$

Now, if L is a characteristic length scale of the fracture and w_{max} a characteristic width, then

$$\delta_l = \frac{w_{max}}{L} \ll 1.$$

With this we have

$$\int_{\Gamma} \mathcal{V} \mathbf{e}_3 \cdot \mathbf{n}_F \psi dS = \int_{\Gamma} \partial_t \mathbf{u} \cdot \mathbf{n}_F \psi dS + O(\delta_l)$$

and, by smoothness of the integrand,

$$\int_{\mathcal{C}} \mathcal{V} \partial_{x_3} \psi dx = O(\delta_l).$$

Hence, to leading order

$$\int_{\mathcal{C}} \rho_{F0} \operatorname{div} (\mathcal{V} \mathbf{e}_3) \psi dx = \rho_{F0} \int_{\Gamma} \partial_t \mathbf{u} \cdot \mathbf{n}_F \psi dS.$$

Then equation (53) becomes

$$\begin{aligned} & \rho_{F0} \int_{\Gamma} \partial_t \mathbf{u} \cdot \mathbf{n}_F \psi dS + \int_{\Gamma} \rho_{F0} \mathbf{q}_{FD} \cdot \mathbf{n}_F \psi dS - \\ & \int_{\mathcal{C}} \rho_{F0} \mathbf{q}_{FD} \cdot \nabla \psi dx = \int_{\mathcal{C}} \rho_{F0} Q_F \psi dx. \end{aligned} \quad (54)$$

Furthermore, for all $\psi \in H^1(\Omega \cup \Gamma \cup \mathcal{C})$, $\psi = 0$ on ∂_{NB} , we have

$$\begin{aligned} & \int_{\Omega} \rho_{R0} (\operatorname{div} (\partial_t \mathbf{u}) \psi - \mathbf{q}_{RD} \cdot \nabla \psi) dx + \int_{\Gamma} \rho_{R0} \mathbf{q}_{RD} \cdot \mathbf{n}_R dS \\ & = \int_{\Omega} \rho_{R0} Q_R \psi dx - \int_{\partial_{D\Omega}} v^{inj} \rho_{R0} \psi dS. \end{aligned} \quad (55)$$

Summing up equations (54) and (55), and using equation (40) or (47) yields

$$\begin{aligned} & \int_{\Omega} \rho_{R0} \operatorname{div} (\partial_t \mathbf{u}) \psi dx - \int_{\Omega} \rho_{R0} \mathbf{q}_{RD} \cdot \nabla \psi dx - \\ & \int_{\mathcal{C}} \rho_{F0} \mathbf{q}_{FD} \cdot \nabla \psi dx + \int_{\Gamma} \rho_{F0} \partial_t \mathbf{u} \cdot \mathbf{n}_F \psi dS = \int_{\mathcal{C}} \rho_{F0} Q_F \psi dx \\ & + \int_{\Omega} \rho_{R0} Q_R \psi dx - \int_{\partial_{D\Omega}} v^{inj} \rho_{R0} \psi dS. \end{aligned} \quad (56)$$

Since

$$\begin{aligned} & \rho_{F0} \int_{\Gamma} \partial_t \mathbf{u} \cdot \mathbf{n}_F \psi dS = \\ & - \rho_{F0} \int_{\Omega} \operatorname{div} (\partial_t \mathbf{u}) \psi dx - \rho_{F0} \int_{\Omega} \partial_t \mathbf{u} \cdot \nabla \psi dx, \end{aligned}$$

equation (56) implies equation (52). \square

To describe the process of hydraulic fracturing one needs to extend the model and add a law allowing for the growth of the fractures. In analogy to fracture theory from solid mechanics, and motivated by experimental evidence, one formulates an explicit equation for the displacement of the tip of the fracture (i.e. points/curves where the curvature of Γ is large). The fracture growth starts if the stress intensity factors exceed a critical value. This critical value is the fracture toughness parameter G_c , which depends on the material properties. It is the so called Griffith's criterion. For a given fracture shape, the stress intensity factors are computed by solving (43)-(47). If they exceed the critical value, one displaces the tip and the fracture grows in that direction. This procedure has found its way to commercial software, see e.g.⁹. It works well when computing the growth of existing fractures, but it fails to describe the creation and/or branching and merging of fractures.

To overcome these difficulties, Francfort and Marigo¹¹ proposed to regularize Griffith's surface energy $G_c \mathcal{H}^2(\mathcal{C})$ by the volume integral

$$\Gamma_{\varepsilon}(\varphi) = G_c \int_B \left(\frac{1}{2\varepsilon} (1 - \varphi)^2 + \frac{\varepsilon}{2} |\nabla \varphi|^2 \right) dx, \quad (57)$$

where $\varepsilon > 0$ is a (small) regularization parameter. In classical fracture mechanics G_c corresponds to the critical energy release rate. Further, φ is the phase field variable or order-parameter. Intuitively, φ is a regularization of $1 - \chi_{\mathcal{C}} = \chi_{\Omega}$. In the classical work of Francfort and Marigo¹¹

it was shown that solutions of the problem based on (57) converge (in the sense of Γ -convergence) to a solution of the original Griffith's formulation.

As in²⁵ the main purpose of this paper is to generalize the approach of Francfort and Marigo to hydraulic fracturing, when the fracture \mathcal{C} is filled with a fluid and when Ω is occupied by a fluid filled porous medium. It is important to note that we are dealing with upscaled equations and conditions. As a consequence, the physical meaning of – in particular – the coupling (46)-(47) is not fundamentally understood in the sense that it has not been derived from a proper upscaling or homogenization procedure.

The phase-field unknown φ is introduced through a regularized elastic energy functional, that is minimized for given pressure field. Then, after the form of $\Gamma_\varepsilon(\varphi)$ yields that $\text{meas}\{(x, t) \in B \times (0, T) \mid \varphi(x, t) \leq a\} \leq C(a)\varepsilon$, for every $a \in (0, 1)$. For more details see Corollary 2 from²⁶. Therefore the parameter ε represents the characteristic length scale and formally the crack behaves as a surface when $\varepsilon \rightarrow 0$.

Throughout the analysis we impose the crack irreversibility constraint (i.e. a condition on the entropy):

$$\partial_t \varphi \leq 0. \quad (58)$$

This means that we restrict ourselves to cracks that grow in time. Since φ regularizes χ_Ω , condition (58) implies $\varphi \leq 1$.

Since the formation of hydraulic cracks is fully dissipative in nature, there is no energy minimization principle to be used for the full phase field formulation (i.e. including the pressure equation). Therefore the key point of our approach is to formulate an energy functional in terms of the displacement \mathbf{u} and phase field φ only, that is for given pressure p . This energy functional contains the presence of fractures through expression (57).

Following the seminal work of Biot⁴, we consider the free isothermal energy density of a poro-elastic system. In the case of incompressible grains and an incompressible fluid it reads

$$W = \frac{1}{2} \mathcal{G} e(\mathbf{u}) : e(\mathbf{u}). \quad (59)$$

The idea is to generalize this energy and to replace it by a "phase field" free energy that takes into the account the following effects:

- Degradation of the elastic properties in the fracture. This is described by multiplying the Gassmann tensor \mathcal{G} by the function $A = A(\varphi)$ satisfying

$$\begin{cases} A : & \text{smooth and non-decreasing,} \\ A(0) = k > 0, & \text{with } k \ll \varepsilon, A(1) = 1. \end{cases} \quad (60)$$

A typical choice is $A(\varphi) = (1 - k)\varphi^2 + k$.

- The global permeability

$$\chi_\Omega \frac{\mathbb{K}k_R(n)}{\eta_R} + \chi_C \frac{\mathbb{K}_F}{\eta_F}$$

is replaced by the interpolated version

$$\mathbb{K}_{eff}(n, \varphi) = \varphi_+ \frac{\mathbb{K}k_R(n)}{\eta_R} + (1 - \varphi_+) \frac{\mathbb{K}_F \rho_{F0}}{\eta_F \rho_{R0}}. \quad (61)$$

- The porosity expression (22) is replaced by

$$n(\varphi, \text{div } \mathbf{u}) = 1 - (1 - n_0)\varphi_+^2 e^{-\text{div } \mathbf{u}}. \quad (62)$$

This expression reflects the pressure of a damaged zone and the fracture in the sense that it describes a smooth transition from $n = 1$ in \mathcal{C} to $n = 1 - (1 - n_0)e^{-\text{div } \mathbf{u}}$ in Ω .

In the above expressions we write φ_+^2 instead of φ . Of course all coefficients A , \mathbb{K}_{eff} and n are naturally defined on $[0, 1]$. But for φ we only have the upper bound $\varphi \leq 1$. Therefore, we replace the values of the coefficients for $\varphi \leq 0$ by their value at $\varphi = 0$. For an elaborate discussion regarding the above sketched approach, we refer to²³ and further comments below.

Our new 'phase-field' free energy density including fractures is now

$$W_\varepsilon = \frac{1}{2} A(\varphi_+) \mathcal{G} e(\mathbf{u}) : e(\mathbf{u}) + G_c \left(\frac{1}{2\varepsilon} (1 - \varphi)^2 + \frac{\varepsilon}{2} |\nabla \varphi|^2 \right). \quad (63)$$

At this point, we note that the phase field modification of the pressure equation (52) has to be written in a way that the free energy W_ε is conserved.

The phase field unknown φ describes a smooth transition from the fracture zone to the poroelastic zone. For the fracture spreading it is crucial to accurately model the location of the interface which has to enter the phase field equation in a correct way.

Our strategy is to generalize the well-established approach from fracture mechanics.

The elastic part phase field energy functional

For the moment we suppose a given pressure, but bear in mind that this pressure is linked to the displacement and the phase-field unknown. Then we borrow the energy functional from fracture theory of solid mechanics which we modify for the spatial porosity changes. As in [Coussy (2004)]⁸, Sec. 4.4.2., we add to the energy functional a cross term involving the integral of the product between the pressure and the porosity change. This is the main difference with the approach of the simplified case in²³ and²⁴. Due to the complexity of our model, it is not clear that we will be able to prove the nonnegativity of φ . Changing the pressure cross term to $\int_B \varphi \nabla p \cdot \mathbf{u} \, dx$ is likely to give nonzero values in the domain where φ is negative. This is not admissible. Using φ_+ instead of φ is also unsatisfactory, since the energy functional would not be C^1 with respect to φ . The lack of regularity could lead to complications in the numerical simulations. Our approach is to use the function φ_+^2 instead of φ . For $0 \leq \varphi \leq 1$, the choice between φ_+^2 and φ_+ in the pressure cross term does not affect the phase field approximation. If $\varphi = 1 - \chi_C$, the two functions coincide. Inserting the phase field unknown

into the variational equation (51) yields the energy functional

$$\begin{aligned} \mathcal{E}_\varepsilon(\mathbf{u}, \varphi) = & \int_B \frac{1}{2} A(\varphi_+) \mathcal{G}e(\mathbf{u}) : e(\mathbf{u}) \, dx - \\ & \int_{\partial_N B} (\boldsymbol{\tau} \cdot \mathbf{u} + p u_n) \, dS + \int_B \left(\frac{\rho_{F0}}{\rho_{R0}} \varphi_+^2 \nabla p + \right. \\ & \left. (1 - \frac{\rho_{F0}}{\rho_{R0}}) \nabla(\varphi_+^2 p) \cdot \mathbf{u} \, dx + \right. \\ & \left. G_c \int_B \left(\frac{1}{2\varepsilon} (1 - \varphi)^2 + \frac{\varepsilon}{2} |\nabla \varphi|^2 \right) \, dx. \right. \end{aligned} \quad (64)$$

Note that the decomposition of the ∇p corresponds to the pressure equation (52).

Calculating Fréchet's derivatives of $\mathcal{E}_\varepsilon(\mathbf{u}, \varphi)$ with respect to \mathbf{u} and φ gives the corresponding PDEs for these unknowns. For details we refer to²⁵, subsections 3.4-3.6. Due to the quasi-static nature of the equations, we restrict ourselves in this work to the time discrete version of the equations: we study an incremental formulation in the next section.

An incremental formulation of the fully-coupled nonlinear system

In the incremental formulation, we replace time derivatives by their discrete versions:

$$\begin{aligned} \partial_t \varphi & \rightarrow \partial_{\Delta t} \varphi = (\varphi - \Phi) / (\Delta t), \\ \partial_t \mathbf{u} & \rightarrow \partial_{\Delta t} \mathbf{u} = (\mathbf{u} - \mathbf{U}) / (\Delta t), \end{aligned}$$

where $\Delta t > 0$ is the time step and where Φ and \mathbf{U} are, respectively, values of the phase field variable and displacement from the previous time step.

The entropy condition (58), imposed in its discretized form, becomes an obstacle condition. It is linked to a convex set K :

$$K = \{\psi \in H^1(B) \mid \psi \leq \Phi \leq 1 \text{ a.e. on } B\}. \quad (65)$$

The sources/sinks and leak terms in the pressure equations are written as the global term

$$\tilde{q} = Q_R \varphi_+ + \frac{\rho_{F0}}{\rho_{R0}} (1 - \varphi_+) Q_F,$$

and the permeability $\tilde{\mathbb{K}}_{eff}$ is taken at porosity n from the current step and the phase field Φ and $\mathbb{K}_F(\Phi)$ from the previous step

$$\begin{aligned} \tilde{\mathbb{K}}_{eff} = & \mathbb{K}_{eff}(n(\varphi_+, \operatorname{div} \mathbf{u}), \Phi_+) = \\ & \Phi_+ \frac{\mathbb{K}_R(n)}{\eta_R} + (1 - \Phi_+) \frac{\mathbb{K}_F(\Phi)}{\eta_F} \frac{\rho_{F0}}{\rho_{R0}}. \end{aligned}$$

The incremental problem, written for the displacement, phase field and pressure, now reads:

$$\begin{aligned} -\operatorname{div} \left(A(\varphi_+) \mathcal{G}e(\mathbf{u}) \right) + \frac{\rho_{F0}}{\rho_{R0}} \varphi_+^2 \nabla p + \\ (1 - \frac{\rho_{F0}}{\rho_{R0}}) \nabla(\varphi_+^2 p) = 0 \quad \text{in } B, \end{aligned} \quad (66)$$

$$-\tilde{\mathbb{K}}_{eff} \nabla p \cdot \mathbf{n} = v^{inj} \text{ and } \mathbf{u} = 0 \text{ on } \partial_D B, \quad (67)$$

$$\mathcal{G}e(\mathbf{u}) \mathbf{n} = \boldsymbol{\tau} + p^{bdry} \mathbf{n} \quad \text{on } \partial_N B, \quad (68)$$

$$\begin{aligned} -G_c \varepsilon \Delta \varphi - \frac{G_c}{\varepsilon} (1 - \varphi) + \frac{1}{2} A(\varphi) \mathcal{G}e(\mathbf{U}) : e(\mathbf{U}) + \\ \mathcal{D}(\varphi) \left(\frac{\rho_{F0}}{\rho_{R0}} \nabla p \cdot \mathbf{U} - (1 - \frac{\rho_{F0}}{\rho_{R0}}) p \operatorname{div} \mathbf{U} \right) \leq 0 \text{ in } B, \end{aligned} \quad (69)$$

$$\partial_{\Delta t} \varphi \leq 0 \quad \text{on } B, \quad (70)$$

$$\begin{aligned} \left(-G_c \varepsilon \Delta \varphi - \frac{G_c}{\varepsilon} (1 - \varphi) + \frac{1}{2} A(\varphi) \mathcal{G}e(\mathbf{U}) : e(\mathbf{U}) + \right. \\ \left. \frac{\rho_{F0}}{\rho_{R0}} \mathcal{D}(\varphi) \nabla p \cdot \mathbf{U} - (1 - \frac{\rho_{F0}}{\rho_{R0}}) \mathcal{D}(\varphi) p \operatorname{div} \mathbf{U} \right) \partial_{\Delta t} \varphi = \\ 0 \text{ in } B, \end{aligned} \quad (71)$$

$$\frac{\partial \varphi}{\partial \mathbf{n}} = 0 \quad \text{on } \partial B, \quad (72)$$

$$\begin{aligned} -\operatorname{div} (\tilde{\mathbb{K}}_{eff} \nabla p) + \frac{\rho_{F0}}{\rho_{R0}} \operatorname{div} (\partial_{\Delta t} (\varphi_+^2 \mathbf{u})) \\ + (1 - \frac{\rho_{F0}}{\rho_{R0}}) \partial_{\Delta t} (\varphi_+^2 \operatorname{div} \mathbf{u}) = \tilde{q} \text{ in } B, \end{aligned} \quad (73)$$

$$p = p^{bdry} \text{ on } \partial_N B. \quad (74)$$

Here (71) is the strong form of Rice' complementarity condition. The functions \mathcal{A} and \mathcal{D} correspond to discrete derivatives of A and φ_+^2 and are given by

$$\mathcal{A}(\varphi) = \frac{A(\varphi_+) - A(\Phi_+)}{\varphi - \Phi} \text{ and } \mathcal{D}(\varphi) = \frac{\varphi_+^2 - \Phi_+^2}{\varphi - \Phi}. \quad (75)$$

For the construction of the Lyapunov functional, it is important to deal with discrete derivatives in (75) and not with A' or $(\varphi_+^2)'$. This will be seen later in the paper.

The modeling and analysis of the case of a linear poroelastic medium was undertaken in²⁵. To the best of our knowledge, the present work is the first result on phase-field modeling of the full system in the case of nonlinear poroelasticity. The mathematical and numerical analysis of the corresponding incremental $\{\mathbf{u}, \varphi, p\}$ -problem has not yet been undertaken in the literature.

Well-posedness of the incremental model

We impose the following on the data of the problem

Hypothesis 1.

\mathcal{G} : positive definite constant rank-4 tensor,

$\tilde{\mathbb{K}}_{eff}$: positively definite and bounded symmetric matrix which depends continuously on n and Φ . Moreover, its ellipticity constant is independent of the arguments.

$\mathbf{U} \in V_U$, $\Phi \in H^1(B)$, $\Phi \leq 1$ a.e. on B ;

$\boldsymbol{\tau} \in L^2(\partial_N B)$, $p^{bdry} \in H^1(B)$,

$v^{inj} \in L^2(\partial_D B)$ and $\tilde{q} \in L^2(B)$.

Here and below V_U and V_P are defined in Proposition 2.

A finite dimensional approximation in space of the incremental problem

Let $\{\psi_r\}_{r \in \mathbb{N}}$ be a basis for $H^1(B)$, $\{\pi_r\}_{r \in \mathbb{N}}$ for V_P and $\{\mathbf{w}^r\}_{r \in \mathbb{N}}$ for V_U . We start by defining a finite dimensional approximation to problem (66)-(74). Let Hypothesis 1 be

satisfied and let $N \in \mathbb{N}$ denote the penalization parameter. Further, let $\tilde{\varphi} = \inf\{1, \varphi_+\}$, $V_U^N = \text{span}\{\mathbf{w}^r\}_{r=1, \dots, N}$, $V_P^N = \text{span}\{\pi_r\}_{r=1, \dots, N}$ and $W^N = \text{span}\{\psi_r\}_{r=1, \dots, N}$.

Definition 3. (Penalized approximation). *The triple $\{\mathbf{u}^N, \varphi^N, p^N\}$, with $\mathbf{u}^N = \sum_{r=1}^N a_r \mathbf{w}^r$, $p^N = p^{bdry} + \sum_{r=1}^N d_r \pi_r$ and $\varphi^N = \Phi + \sum_{r=1}^N b_r \psi_r$, is called a finite dimensional approximate solution of problem (66)-(74) if it satisfies the discrete variational formulation*

$$\begin{aligned} & \int_B (A(\tilde{\varphi}^N) \mathcal{G}e(\mathbf{u}^N) : e(\mathbf{w}^r) + \frac{\rho_{F0}}{\rho_{R0}} (\tilde{\varphi}^N)^2 \nabla p^N \cdot \mathbf{w}^r + \\ & (1 - \frac{\rho_{F0}}{\rho_{R0}}) \nabla((\tilde{\varphi}^N)^2 p^N) \cdot \mathbf{w}^r) dx = \\ & \int_{\partial_N B} (\tau \cdot \mathbf{w}^r + p^{bdry} \mathbf{w}_n^r) dS, \quad \forall r = 1, \dots, N; \quad (76) \\ & G_c \int_B (-\frac{1}{\varepsilon} (1 - \varphi^N) \psi_r + \varepsilon \nabla \varphi^N \cdot \nabla \psi_r) dx \\ & + \int_B \delta(\varphi^N - \Phi)_+ \psi_r dx + \frac{1}{2} \int_B \mathcal{A}(\tilde{\varphi}^N) \mathcal{G}e(\mathbf{U}) : e(\mathbf{U}) \psi_r dx \\ & + \int_B \mathcal{D}(\tilde{\varphi}^N) (\frac{\rho_{F0}}{\rho_{R0}} \nabla p^N \cdot \mathbf{U} - (1 - \frac{\rho_{F0}}{\rho_{R0}}) p^N \text{div } \mathbf{U}) \psi_r dx \\ & = 0, \quad \forall r = 1, \dots, N; \quad (77) \\ & \int_B (\frac{\rho_{F0}}{\rho_{R0}} \text{div}((\tilde{\varphi}^N)^2 \mathbf{u}^N) + (1 - \frac{\rho_{F0}}{\rho_{R0}}) (\tilde{\varphi}^N)^2 \text{div } \mathbf{u}^N) \pi_r dx \\ & + \Delta t \int_B \tilde{\mathbb{K}}_{eff} \nabla p^N \cdot \nabla \pi_r dx = \Delta t \int_B \tilde{q} \pi_r dx \\ & + \Delta t \int_{\partial_D B} v^{inj} \pi_r dS + \frac{\rho_{F0}}{\rho_{R0}} \int_B \text{div}(\Phi_+^2 \mathbf{U}) \pi_r dx \\ & + (1 - \frac{\rho_{F0}}{\rho_{R0}}) \int_B \Phi_+^2 \text{div } \mathbf{U} \pi_r dx, \quad \forall r = 1, \dots, N, \quad (78) \end{aligned}$$

with given $\{\mathbf{U}, \Phi\} \in V_U \times H^1(B)$ and

$$\begin{aligned} \mathcal{A}(\tilde{\varphi}^n) &= \frac{A(\tilde{\varphi}^n) - A(\Phi_+)}{\varphi^n - \Phi} \\ \text{and } \mathcal{D}(\tilde{\varphi}^n) &= \frac{(\tilde{\varphi}^n)^2 - \Phi_+^2}{\varphi^n - \Phi}, \quad n = 1, \dots, N. \quad (79) \end{aligned}$$

Proposition 4. *Suppose Hypothesis 1 holds. Then there exists a finite dimensional approximate solution of problem (76)-(78) in the sense of Definition 3. This approximation satisfies, for $N \in \mathbb{N}$ and $\delta \in \mathbb{R}_+$,*

$$\begin{aligned} G_c \int_B (\frac{(\varphi^N)^2}{\varepsilon} + \varepsilon |\nabla \varphi^N|^2) dx + \int_B \delta(\varphi^N - \Phi)_+^2 dx \\ + \|\mathbf{u}^N\|_{H^1(B)^3}^2 + \|p^N\|_{H^1(B)}^2 \leq C, \quad (80) \end{aligned}$$

where C is dependent on N and δ .

Proof. (of Proposition 4). The proof goes along the same lines as the proof of Proposition 2 from²⁵. The fact that the permeability tensor $\tilde{\mathbb{K}}_{eff}$ now depends on the porosity n and Φ as well does not change the estimates. The fact that the fluid is incompressible needs attention. When $\partial B = \partial_D B$, the usual compatibility condition on the data is necessary for the existence of a solution. However, since we are dealing with mixed boundary conditions for the pressure which is given on $\partial_N B$, one can use Poincaré's inequality. This yields a coercivity argument similar to (68) from²⁵. \square

Existence of a solution to the incremental problem

In this section we show existence of a weak solution:

Theorem 5. *Let Hypothesis 1 holds true. Then there exists at least one variational solution $\{\mathbf{u}, \varphi, p\} \in V_U \times (H^1(B) \cap K) \times V_P$ of problem (66)-(74).*

Proof. By Proposition 4, there exists a finite dimensional solution $\{\mathbf{u}^N, \varphi^N, p^N\}$ of problem (76)-(78), satisfying the a priori estimate (80). Let $\delta = N$. Therefore there exists $\{\mathbf{u}, \varphi, p\}$ and a subsequence, denoted again by the same superscript, such that in the limit $N \rightarrow \infty$

$$\begin{aligned} \{\mathbf{u}^N, \varphi^N, p^N\} &\rightarrow \{\mathbf{u}, \varphi, p\} \text{ weakly in } V_U \times H^1(B) \times V_P, \\ &\text{strongly in } L^q(B)^5, \quad q < 6, \text{ and a.e. on } B. \quad (81) \end{aligned}$$

Obviously $(\varphi^N - \Phi)_+ \rightarrow 0$, as $N \rightarrow \infty$, and $\varphi \in K$.

Since $\tilde{\varphi}^N \rightarrow \tilde{\varphi}$ strongly in $L^q(B)$, for all $q < +\infty$, we can pass to the limit in equation (76) directly. Therefore, the triple $\{\mathbf{u}, \varphi, p\}$ satisfies equation (66) and boundary condition (68).

Passing to the limit $N \rightarrow \infty$ in equation (77) is along the same lines as in the proof of Theorem 1 from²⁵ and we conclude that $\{\mathbf{u}, \varphi, p - p^{bdry}\} \in V_U \times (H^1(B) \cap K) \times V_P$ is a solution to the inequality (69) and (70). In addition the Rice condition (71) holds.

Concerning the variational equation (78), the permeability $\tilde{\mathbb{K}}_{eff}$ depends on n , which is a function of $\text{div } \mathbf{u}$ and φ . Therefore, we need some more work to conclude that the triple $\{\mathbf{u}, \varphi, p\}$ satisfies equation (73) and boundary conditions (67), (74). It is tempting to follow the approach from⁵, who used a result from²⁸ on the strong H^1 -convergence of the displacement if the pressure converges strongly in L^2 . However, that result was established for the continuous space setting. Here we give a self-contained proof for the convergence of the Galerkin approximation.

Let $\Pi^N : V_U \rightarrow V_U^N$ be a projector such that $\Pi^N v \rightarrow v$ in $H^1(B)^3$, as $N \rightarrow +\infty$. Note that, by (81), $\mathbf{u}^N - \Pi^N \mathbf{u} \rightarrow 0$ strongly in $L^2(B)^3$ and weakly in $H^1(B)^3$, as $N \rightarrow +\infty$. Let $\lambda = \frac{\rho_{F0}}{\rho_{R0}}$. Then we have

$$\begin{aligned} & \int_B (A(\tilde{\varphi}^N) \mathcal{G}e(\mathbf{u}^N) : e(\mathbf{u}^N - \Pi^N \mathbf{u}) + (\lambda (\tilde{\varphi}^N)^2 \nabla p^N \\ & + (1 - \lambda) \nabla((\tilde{\varphi}^N)^2 p^N)) \cdot (\mathbf{u}^N - \Pi^N \mathbf{u})) dx = \\ & \int_{\partial_N B} (\tau \cdot (\mathbf{u}^N - \Pi^N \mathbf{u}) + p^{bdry} (\mathbf{u}^N - \Pi^N \mathbf{u}) \cdot \mathbf{n}) dS, \quad (82) \end{aligned}$$

$$\begin{aligned} & \int_B (A(\tilde{\varphi}) \mathcal{G}e(\Pi^N \mathbf{u}) : e(\mathbf{u}^N - \Pi^N \mathbf{u}) + (\lambda (\tilde{\varphi})^2 \nabla p \\ & + (1 - \lambda) \nabla((\tilde{\varphi}^N)^2 p^N)) \cdot (\mathbf{u}^N - \Pi^N \mathbf{u})) dx \\ & = \int_{\partial_N B} (\tau \cdot (\mathbf{u}^N - \Pi^N \mathbf{u}) + p^{bdry} (\mathbf{u}^N - \Pi^N \mathbf{u}) \cdot \mathbf{n}) dS + \\ & \int_B (A(\tilde{\varphi}) \mathcal{G}e(\Pi^N \mathbf{u} - \mathbf{u}) : e(\mathbf{u}^N - \Pi^N \mathbf{u})) dx. \quad (83) \end{aligned}$$

Subtracting equalities (82)-(83) yields

$$\begin{aligned} & \int_B A(\tilde{\varphi}^N) \mathcal{G}e(\mathbf{u}^N - \Pi^N \mathbf{u}) : e(\mathbf{u}^N - \Pi^N \mathbf{u}) \, dx = \\ & \int_B (A(\tilde{\varphi}^N) - A(\tilde{\varphi})) \mathcal{G}e(\Pi^N \mathbf{u}) : e(\mathbf{u}^N - \Pi^N \mathbf{u}) \, dx + \\ & \lambda \int_B ((\tilde{\varphi})^2 \nabla p - (\tilde{\varphi}^N)^2 \nabla p^N) \cdot (\mathbf{u}^N - \Pi^N \mathbf{u}) \, dx \\ & - (1 - \lambda) \int_B ((\tilde{\varphi})^2 p - (\tilde{\varphi}^N)^2 p^N) \operatorname{div}(\mathbf{u}^N - \Pi^N \mathbf{u}) \, dx \\ & - \int_B (A(\tilde{\varphi}) \mathcal{G}e(\Pi^N \mathbf{u} - \mathbf{u}) : e(\mathbf{u}^N - \Pi^N \mathbf{u}) \, dx. \quad (84) \end{aligned}$$

Equality (84) allows us to conclude that

$$\begin{aligned} \mathbf{u}^N - \Pi^N \mathbf{u} & \rightarrow 0 \quad \text{in } H^1(B)^3 \quad \text{and} \\ \operatorname{div} \mathbf{u}^N & \rightarrow \operatorname{div} \mathbf{u} \quad \text{strongly in } L^2(B), \quad \text{as } N \rightarrow +\infty. \end{aligned}$$

With the above strong convergence, passing to the limit $N \rightarrow +\infty$ in equation (78) is straightforward and proof of the theorem is complete. \square

Lyapunov functional for the incremental problem

In this subsection we show that the "phase field" free energy (63) acts as a Lyapunov functional for the incremental (time discrete) problem (66)-(74).

In (66)-(74), where the discrete time step enters as parameter, one finds the triple $\{\mathbf{u}, \varphi, p\}$ from the "initial values" $\{\mathbf{U}, \Phi\}$. The idea is to repeat the procedure for an arbitrary ($N \in \mathbb{N}$) number of times to obtain a time discretized approximation of the original quasi-static equations.

Assuming that Δt is the same for each step, we introduce the discrete times

$$t_j = j\Delta t, \quad j = 0, \dots, N.$$

For $j = 1, \dots, N$, let $\{\mathbf{u}, \varphi, p\}(t_j)$ denote the solution of problem (66)-(74) with

$$\Phi = \varphi(t_{j-1}), \quad \mathbf{U} = \mathbf{u}(t_{j-1})$$

and where

$$\mathbf{u}(0) \in V_U \quad \text{and} \quad \varphi(0) \in H^1(B), \quad \Phi \leq 1 \quad (\text{a.e.}) \quad \text{in } B.$$

With these values, we define the approximate solution by

$$\{\mathbf{u}(t), \varphi(t), p(t)\} = \{\mathbf{u}(t_j), \varphi(t_j), p(t_j)\}$$

for $t_j \leq t < t_{j+1}$ and for $j = 0, \dots, N-1$.

In the following justification, we suppose for simplicity $p^{bdry} = 0$. Having a non-homogeneous pressure boundary condition does not pose an essential problem but leads to long and cumbersome expressions.

Next, introduce the Lyapunov functional at $t_N = N\Delta t$

$$\begin{aligned} J^N & = \frac{1}{2} \int_B \left(A(\tilde{\varphi}_N) \mathcal{G}e(\mathbf{u}_N) : e(\mathbf{u}_N) + G_c(\varepsilon |\nabla \varphi_N|^2 + \right. \\ & \left. \frac{1}{\varepsilon} (1 - \varphi_N)^2) \right) dx - \int_{\partial_N B} \tau(t_N) \cdot \mathbf{u}_N \, dS. \quad (85) \end{aligned}$$

Then we have the following result:

Theorem 6. *Suppose Hypothesis 1 holds and, in addition, $p^{bdry} = 0$. Then we have the estimate:*

$$\begin{aligned} J^N + \Delta t \sum_{j=0}^{N-1} \int_B \tilde{\mathbb{K}}_{eff}(t_j) \nabla p(t_{j+1}) \cdot \nabla p(t_{j+1}) \, dx & \leq J^0 + \\ \Delta t \sum_{j=0}^{N-1} \int_{\partial_N B} \partial_{\Delta t} \tau(t_{j+1}) \cdot \mathbf{u}(t_{j+1}) \, dS & \\ + \Delta t \sum_{j=0}^{N-1} \int_{\partial_D B} v^{inj}(t_{j+1}) p_{j+1} \, dS & \\ + \Delta t \sum_{j=0}^{N-1} \int_B \tilde{q}(t_{j+1}) p_{j+1} \, dx, & \quad (86) \end{aligned}$$

where J^0 is calculated using the initial values of the unknowns.

Proof. The proof goes along the same lines as the proof of Theorem 2 from²⁵. \square

Numerical tests

We substantiate our modeling through some numerical tests. First, the discretization and solution algorithm are briefly described. Afterwards, two 2d configurations yielding six test cases are presented.

General comments on the discretization, solution algorithm and programming code

For spatial discretization we use a Galerkin finite element scheme on quadrilaterals with bilinear shape functions. Temporal discretization is based on the backward Euler scheme. The nonlinear system is treated with Newton's method in which a GMRES (generalized minimal residual) method with algebraic block-preconditioning is employed for solving the linear equations. Here we notice that the displacement/phase-field system is very challenging to be solved when treated in a fully monolithic fashion, e.g.,^{13,30}. For this reason, we extrapolate φ in the u -equation (76) as suggested in¹⁶.

The programming code is an extension of our previous version²⁵ using the finite element package deal.II². All principle details on Newton's method and the Jacobian matrix can be found therein. The novelty from the algorithmic point of view is to incorporate the nonlinear permeability in the pressure equation (78).

Discretization and linearization of the pressure equation

We now concentrate on the linearization of the pressure equation (78). As previously mentioned, the displacement/phase-field system (76) - (77) has been discussed in detail in other studies, e.g.,²⁵.

In weak form, the incremental pressure on the spatially continuous level reads:

$$\begin{aligned} A_p(\mathcal{U})(\pi) &:= -\frac{\rho_{F0}}{\rho_{R0}} \int_B \operatorname{div}(\Phi_+^2 \mathbf{U}) \pi \, dx + \\ &\int_B \left(\frac{\rho_{F0}}{\rho_{R0}} \operatorname{div}((\tilde{\varphi})^2 \mathbf{u}) + \left(1 - \frac{\rho_{F0}}{\rho_{R0}}\right) \tilde{\varphi}^2 \operatorname{div} \mathbf{u} \right) \pi \, dx \\ &+ \Delta t \int_B \tilde{\mathbb{K}}_{eff} \nabla p \cdot \nabla \pi \, dx - \Delta t \int_B \tilde{q} \pi \, dx \\ &- \Delta t \int_{\partial_D B} v^{inj} \pi \, dS - \int_B \left(1 - \frac{\rho_{F0}}{\rho_{R0}}\right) \Phi_+^2 \operatorname{div}(\mathbf{U}) \pi \, dx, \end{aligned}$$

where $\mathcal{U} := \{\mathbf{u}, \varphi, p\}$. When we derive the directional derivative we first remark that the first and the last two terms are given data and previous time step solutions. We recall that $\tilde{\mathbb{K}}_{eff}$ is defined in (61). Next, $k_R(n) := k_R(n(\mathbf{u}, \varphi))$ is defined in (4). Then, $n := n(\mathbf{u}, \varphi)$ is defined in (62). Applying several times the chain rule to the first three terms in $A_p(\mathcal{U})(\pi)$, we obtain:

$$\begin{aligned} A'_p(\mathcal{U})(d\mathcal{U}, \pi) &= \frac{\rho_{F0}}{\rho_{R0}} \int_B \operatorname{div}(\tilde{\varphi}^2 d\mathbf{u} + 2\mathbf{u}\varphi_+ H(1-\varphi)d\varphi) \pi \, dx + \\ &\left(1 - \frac{\rho_{F0}}{\rho_{R0}}\right) \int_B (\tilde{\varphi}^2 \operatorname{div} d\mathbf{u} + 2 \operatorname{div} \mathbf{u} \varphi_+ H(1-\varphi)d\varphi) \pi \, dx \\ &+ \Delta t \int_B \left(\tilde{\mathbb{K}}'_{eff}(d\mathbf{u}) \nabla p + \tilde{\mathbb{K}}_{eff} dp \right) \cdot \nabla \pi \, dx, \end{aligned}$$

with $d\mathcal{U} := \{d\mathbf{u}, d\varphi, dp\}$. In $\tilde{\mathbb{K}}_{eff}$ we time-lag the phase-field variable and obtain:

$$\tilde{\mathbb{K}}_{eff} = \tilde{\mathbb{K}}_{eff}(n(\mathbf{u}, \varphi), \Phi_+) = \Phi_+ \frac{k_R(n)}{\eta_R} + (1 - \Phi_+) \frac{k_F}{\eta_F}.$$

The directional derivative reads:

$$\begin{aligned} \tilde{\mathbb{K}}'_{eff}(n, \Phi_+)(d\mathbf{u}) &= \frac{dK_{eff}}{dn} \frac{dn}{d(\mathbf{u}, \varphi)} \\ &= \Phi_+ \frac{k'_R(n)(d\mathbf{u})}{\eta_R} (1 - n_0) e^{-\operatorname{div} \mathbf{u}(\varphi_+^2 \operatorname{div} d\mathbf{u} - 2\varphi_+ d\varphi)} \end{aligned}$$

where $(k_R(n))'(d\mathbf{u})$ is left for the reader using again the chain and quotient rules.

Remark 7. Spatial discretization is later indicated by adding the index h .

Newton's method

We now formulate Newton's method for the full system given in Definition 3. Here, the semi-linear form $A(\cdot)(\cdot)$ describes the entire variational formulation in which the three subsystems are summed up.

Algorithm 1. Newton iteration of the fully-coupled system. At a given time level; repeat the Newton iterations for $k = 0, 1, 2, \dots$:

1. Find $d\mathcal{U}_k^h := \{d\mathbf{u}_k^h, d\varphi_k^h, dp_k^h\}$ by solving the linear system

$$A'(\mathcal{U}_k^h)(d\mathcal{U}_k^h, \Psi^h) = -A(\mathcal{U}_k^h)(\Psi^h), \quad (87)$$

for all $\Psi \in V_U^h \times W^h \times V_P^h$.

2. Find a step size $0 < \omega \leq 1$ using line search to get

$$\mathcal{U}_{k+1}^h = \mathcal{U}_k^h + \omega d\mathcal{U}_k^h,$$

such that $A(\mathcal{U}_{k+1}^h)(\Psi^h) < A(\mathcal{U}_k^h)(\Psi^h)$.

Finish the Newton loop if the stopping criteria is fulfilled:

$$|A(\mathcal{U}_k^h)(\Psi^h)| < \text{TOL}, \quad \text{TOL} > 0.$$

Remark 8. Inside Newton's method the semi-linear form is composed as the sum of the single variational formulation of the displacement, phase-field and pressure equations. We notice that the pressure equation has been previously derived and details on the displacement/phase-field system can be found in²⁵.

Remark 9. The crack irreversibility constraint is realized with a primal-dual active set strategy that has been worked out for phase-field fracture in¹⁶. The result is a combined semi-smooth Newton method that solves for both the constraint and the nonlinear problem. The algorithm for the linear Biot case is stated in detail in²⁵.

Parameters for the numerical tests

All parameters are summarized in Table 2.

S	QUANTITY	VALUE	UNIT
k	bulk regularization	10^{-12}	m
ε	phase-field regularization	$2h$	m
h	discretization parameter	0.044	m
Δt	time step size	0.01	s
T	time interval	50	s
k_{ref}	Reference permeability	10^{-10}	Darcy
η_R	Reservoir fluid viscosity	10^{-3}	kg/m sec
η_F	Fracture fluid viscosity	10^{-3}	kg/m sec
p_{pb}	Injection pressure	10^{-8}	Pa
E	Young's modulus	10^8	Pa
ν_S	Poisson's ratio	0.2	
G_c	Critical energy release rate	1	J/m ²

Table 2. Parameters for the numerical examples

The point source injection is modeled as $\tilde{q} = p_{pb} \frac{d}{\pi} \exp(-C_0 d * (x - x_0)^2)$ with $d = 10000$ 1/Pa, $C_0 = 1$ Pa/m² and $x_0 = (2, 2)$ m. The fracture permeability is computed as $K_F \sim w^2/12\eta_F$ where w is the width of the fracture. The domain is $\Omega = (0, 4)^2$ with boundary $\partial\Omega$.

Boundary conditions and test cases

We split the boundary as $\partial B = \partial_l B \cup \partial_r B \cup \partial_b B \cup \partial_t B$ into left, right, bottom, and top boundary sections. We design two examples, a straight fracture and two fractures, yielding six test cases:

- Case 1 (straight fracture): $u = 0$ and $p = 0$ on ∂B ;
- Case 2 (two fractures): $u = 0$ and $p = 0$ on ∂B ;
- Case 3 (straight fracture): $u = 0$ and $\nabla p \cdot \mathbf{n} = 0$ on $\partial_{l,r} B$ and $\mathcal{G}e(\mathbf{u})\mathbf{n} = \tau + p^{bdry} \mathbf{n}$ and $p = 0$ on $\partial_{b,t} B$ with $\tau = (0, 0)$;
- Case 4 (two fractures): $u = 0$ and $\nabla p \cdot \mathbf{n} = 0$ on $\partial_{l,r} B$ and $\mathcal{G}e(\mathbf{u})\mathbf{n} = \tau + p^{bdry} \mathbf{n}$ and $p = 0$ on $\partial_{b,t} B$ with $\tau = (0, 0)$;

- Case 5 (straight fracture): $u = 0$ and $\nabla p \cdot \mathbf{n} = 0$ on $\partial_{l,r}B$ and $\mathcal{G}e(\mathbf{u})\mathbf{n} = \tau + p^{bdry}\mathbf{n}$ and $p = 0$ on $\partial_{b,t}B$ with $\tau = (0, -1.0 \times 10^5)$ on ∂_bB and $\tau = (0, 1.0 \times 10^5)$ on ∂_tB
- Case 6 (two fractures): $u = 0$ and $\nabla p \cdot \mathbf{n} = 0$ on $\partial_{l,r}B$ and $\mathcal{G}e(\mathbf{u})\mathbf{n} = \tau + p^{bdry}\mathbf{n}$ and $p = 0$ on $\partial_{b,t}B$ with $\tau = (0, -1.0 \times 10^5)$ on ∂_bB and $\tau = (0, 1.0 \times 10^5)$ on ∂_tB

With regard to the boundary conditions, we notice that²² also used $p = 0$ for a related test using the linear Biot model and¹⁵ used mixed boundary conditions with traction forces of a similar order as we employed in our simulations. We furthermore notice that in the cases 2,4 and 6, the fluid is only injected into the horizontal fracture. The vertical fracture is empty at the initial time. This can be seen by observing the pressure field in Figure 10.

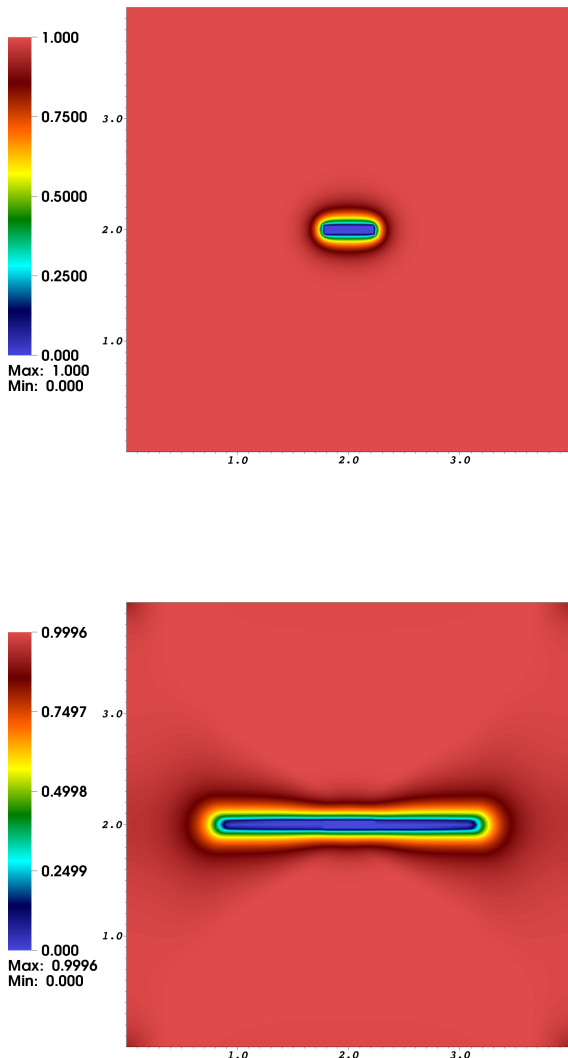


Figure 4. A straight fracture (case 5): Fracture pattern displayed in terms of the phase-field variable φ at $T = 0.01s$ and $T = 0.5s$.

In the following, we focus our attention to the cases 5 and 6 for discussing the phase-field solution, pressure solution,

and crack opening displacements. In fact our findings for the cases 1 and 2 are similar to²⁵ in which we worked with the linear Biot equations. For all six test cases, however, we show the evolution of the minimum and maximum permeabilities in the Figures 6 and 7.

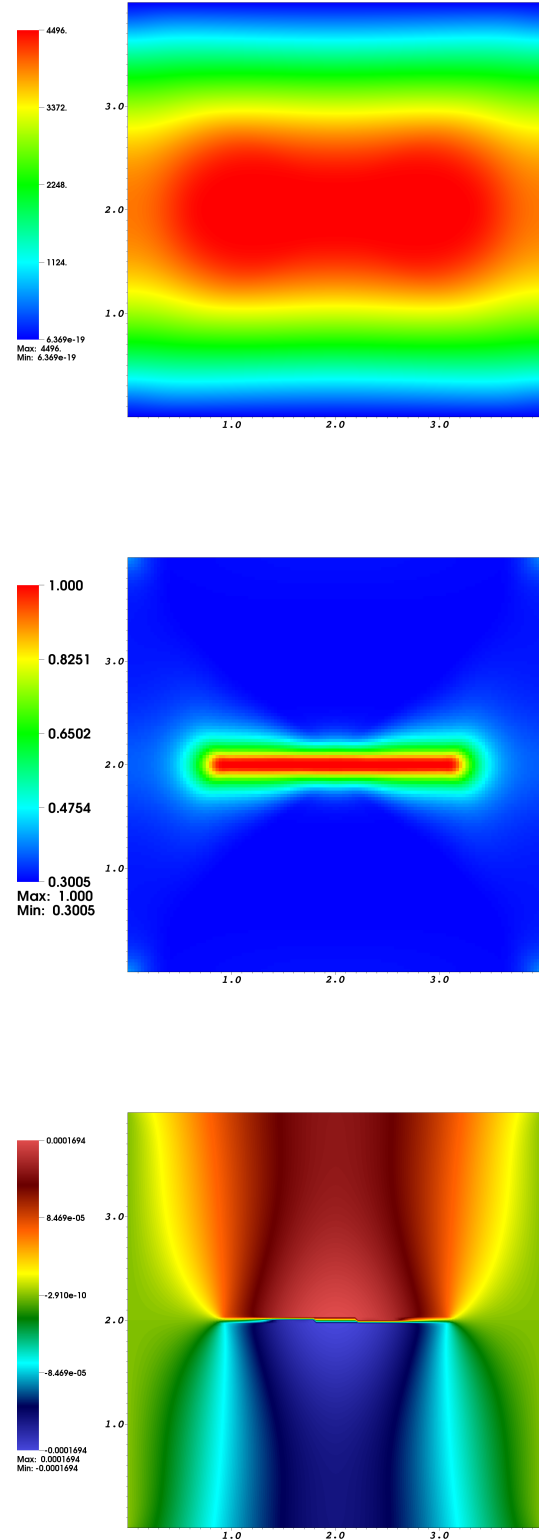


Figure 5. A straight fracture (case 5): pressure, porosity, and u_y displacements at $T = 0.5s$.

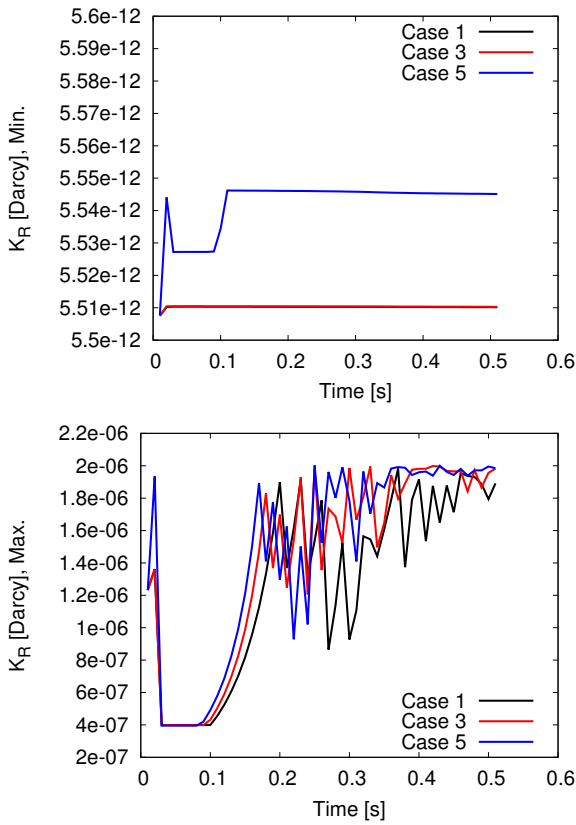


Figure 6. A straight fracture: evolution and values of the minimum and maximum of K_R for the cases 1,3,5.

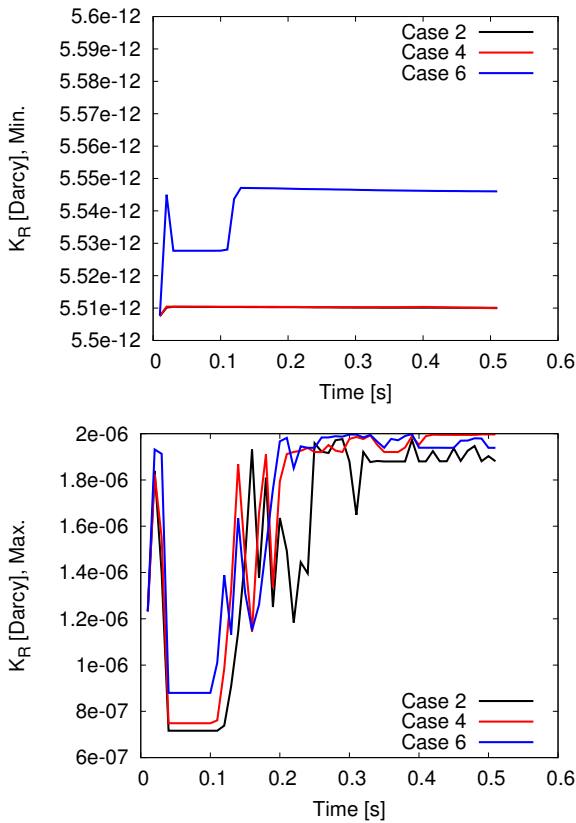


Figure 7. Two fractures: evolution and values of the minimum and maximum of K_R for the cases 2,4,6.

A straight fracture (cases 1,3,5)

In this first example, an initial crack is described with length $l_0 = 0.4$ on $\mathcal{C} = (1.8 - h, 2.2 + h) \times (2 - h, 2 - h) \subset \Omega$. A single-phase fluid with source term q is injected into the middle of the domain in the point $(2, 2)$.

As previously mentioned, we concentrate on results from Case 5. The crack patterns are displayed in Figure 4. The pressure, porosity, and u_y displacements are illustrated in Figure 5. We observe the typical shape of the crack opening displacement; namely zero opening at the tips of the fracture and largest opening in the middle. In Figure 5 (bottom) we clearly see the influence of the nonhomogeneous traction forces. The evolution of the (nonlinear) permeabilities is displayed in Figure 6. Here, case 3 (zero traction force) yields comparable findings to case 1 as we expected. The minimal permeability for non-zero traction forces is higher as it is reasonable.

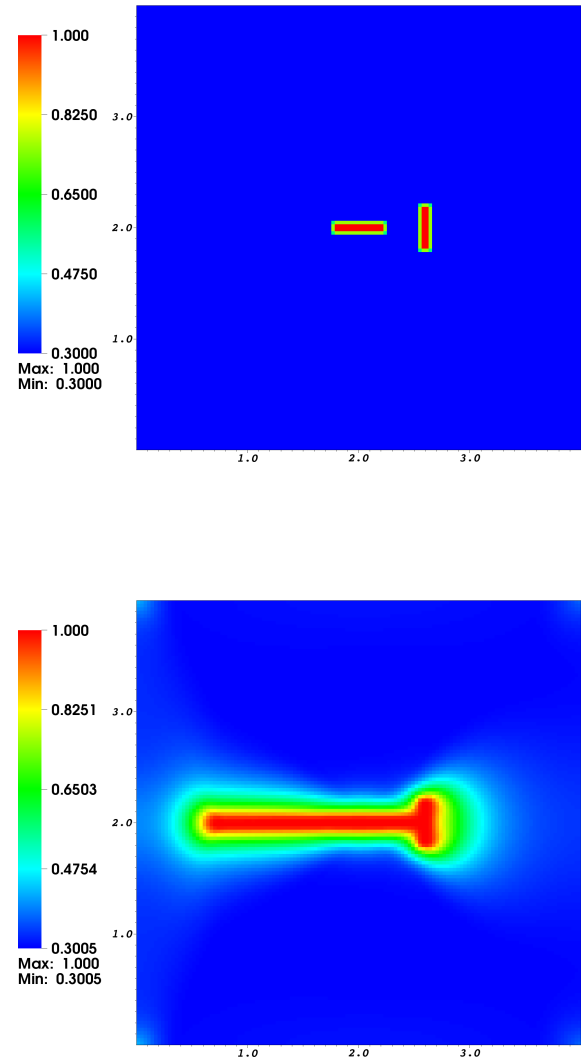


Figure 8. Two fractures (case 6): porosity n at $T = 0.01s$ and $T = 0.5s$.

Two fractures (cases 2,4,6)

In this second test, the domain, boundary conditions and the first fracture (the horizontal one) remain the same as in the first example. We now add a second, vertically-aligned fracture on $(2.6 \pm h, 2.0 \pm 0.2)$. We only do inject a fluid into fracture 1 (like in the first example). Consequently, the second fracture can be seen as a natural non-pressurized fracture.

Analyzing our findings, the following conclusions can be inferred: In Figure 9, we observe the crack pattern evolution and see that only fracture 1 starts propagating because fracture 2 is not pressurized. For case 2 the two fractures join at $T = 0.29s$ and for case 4 at $T = 0.26s$ and case 6 at $T = 0.21s$. The evolution of the minimal and maximal permeabilities is displayed in Figure 7.

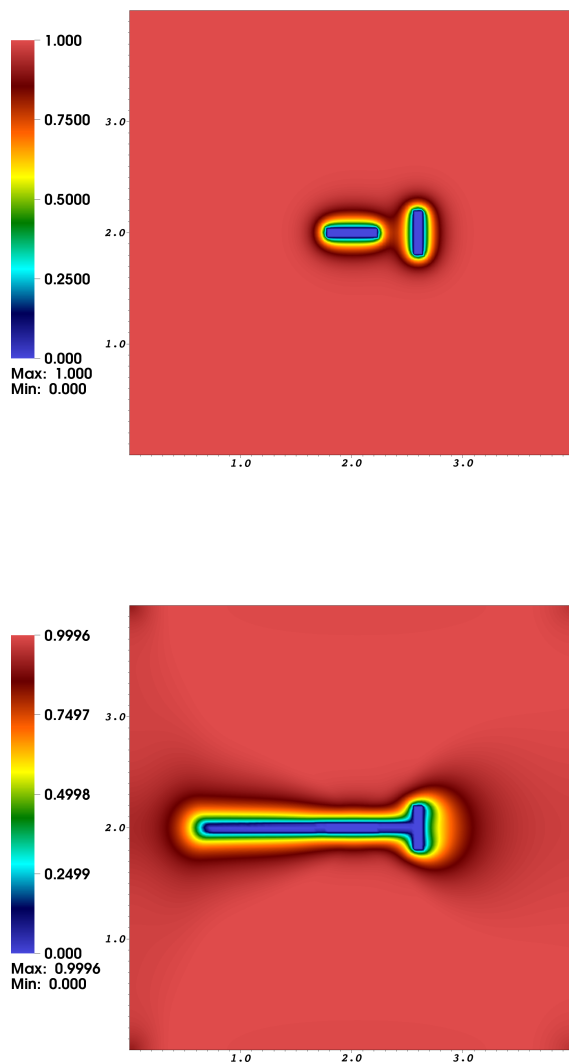


Figure 9. Two fractures (case 6): Fracture pattern displayed in terms of the phase-field variable φ at $T = 0.01s$, and $T = 0.5s$ for both cases.

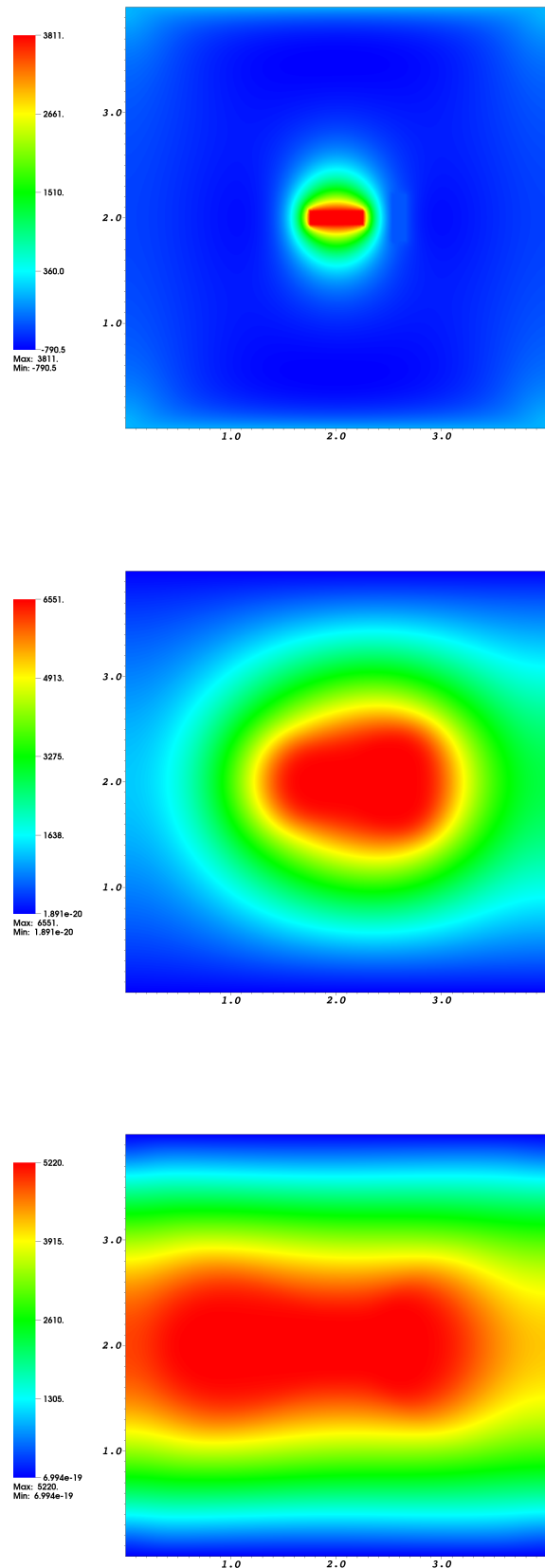


Figure 10. Two fractures (case 6): pressure field at $T = 0.01s$, $T = 0.21 s$ and $T = 0.5s$.

Conclusion

In this work, we derived and analyzed phase-field fracture propagation in a nonlinear incompressible and deformable porous medium. The simulations presented in the article show similarities with the case of a linear poroelastic medium from²⁵. Nevertheless the phase-field variable and pressure profiles seem to be more smooth. This can be justified by the porosity that changes with the solid skeleton compression and phase-field, and also by the permeability depending on the porosity. We envisage to undertake more numerical tests in forthcoming research.

Funding

The research of A.M. was supported in part by the LABEX MILYON (ANR-10-LABX-0070) of Université de Lyon, within the program "Investissements d'Avenir" (ANR-11-IDEX-0007) operated by the French National Research Agency (ANR) and by the Darcy Center during his visits in February and March 2018.

References

- Adachi J, Siebrits E; Peirce A and Desroches J. Computer simulation of hydraulic fractures. *Int J Rock Mech Min Sci* 2007; 44: 739–757.
- Bangerth W, Davydov D, Heister T, Heltai L, Kanschat G, Kronbichler M, Maier M, Turcksin B and Wells D. The deal.II library, version 8.4. *J. Numer. Math.* 2016; **24**: 135–141.
- Bear J and Bachmat Y. *Introduction to Modeling of Transport Phenomena in Porous Media*, Springer Science and Business Media, 1990.
- Biot MA. Mechanics of Deformation and Acoustic Propagation in Porous Media. *J. Appl. Phys.* 1962; 33: 1482.
- Bociu L, Guidoboni G, Sacco R and Webster JT. Analysis of nonlinear poro-elastic and poro-visco-elastic models. *Arch. Ration. Mech. Anal.* 2016; 222: 1445–1519.
- Cajuhi T, Sanavia L and De Lorenzis L. Phase-field modeling of fracture in variably saturated porous media. to appear in *Comput. Mech.* 2017.
- Cao Y, Chen S and Meir AJ. Analysis and numerical approximations of equations of nonlinear poroelasticity. *Discrete Contin. Dyn. Syst. Ser. B* 2013; 18: 1253–1273.
- Coussy O. *Poromechanics*, John Wiley and Sons, 2004.
- Dean RH and Schmidt JH. Hydraulic-Fracture Predictions with a fully coupled geomechanical reservoir simulator. *SPE Journal.* 2009; 14: 707-714.
- Detournay E. Mechanics of Hydraulic Fractures. *Annu. Rev. Fluid Mech.* 2016; 48: 311-39.
- Francfort G A and Marigo J J. Revisiting brittle fracture as an energy minimization problem. *J. Mech. Phys. Solids.* 1998; 46: 1319–1342.
- Ganis B, Girault V, Mear M, Singh G and Wheeler MF. Modeling fractures in a poro-elastic medium. *Oil & Gas Science and Technology - Rev. IFP, Energies nouvelles* 2014; 69: 515-528.
- Gerasimov T and De Lorenzis L. A line search assisted monolithic approach for phase-field computing of brittle fracture. *Comp. Meth. Appl. Mech. Engrg.* 2016; 312: 276 – 303.
- Hamrock BJ, Schmid SR and Jacobson BO. *Fundamentals of fluid film lubrication*. CRC press, 2004.
- Heider Y and Markert B. A phase-field modeling approach of hydraulic fracture in saturated porous media. *Mechanics Research Communications* 2017; 80: 38 – 46.
- Heister T, Wheeler MF and Wick T. A primal-dual active set method and predictor-corrector mesh adaptivity for computing fracture propagation using a phase-field approach. *Comp. Meth. Appl. Mech. Engrg.* 2015; 290: 466 – 495.
- Kaviany M *Principles of heat transfer in porous media*. Springer Science and Business Media, 2012.
- Lee S, Wheeler MF and Wick T. Pressure and fluid-driven fracture propagation in porous media using an adaptive finite element phase field model. *Comp. Meth. Appl. Mech. Engrg.* 2016; 305: 111 – 132.
- Lee S, Wheeler MF and Wick T. Iterative coupling of flow, geomechanics and adaptive phase-field fracture including level-set crack width approaches. *J. Comput. Appl. Math* 2017; 314: 40 – 60.
- Lewis R W and Schrefler B A. *The Finite Element Method in the Static and Dynamic Deformation and Consolidation of Porous Media*. John Wiley and Sons, 1998.
- Miehe C and Mauthe S. Phase field modeling of fracture in multi-physics problems. part iii. crack driving forces in hydro-poro-elasticity and hydraulic fracturing of fluid-saturated porous media. *Comp. Meth. Appl. Mech. Engrg.* 2016; 304: 619 – 655.
- Miehe C, Mauthe S and Teichtmeister S. Minimization principles for the coupled problem of Darcy Biot-type fluid transport in porous media linked to phase field modeling of fracture. *J. Mech. Phys. Solids* 2015; 82: 186 – 217.
- Mikelić A, Wheeler MF and Wick T. A quasistatic phase field approach to pressurized fractures. *Nonlinearity* 2015; 28: 1371-1399.
- Mikelić A, Wheeler MF and Wick T. A phase-field method for propagating fluid-filled fractures coupled to a surrounding porous medium. *SIAM Multiscale Model. Simul.* 2015; 13: 367–398.
- Mikelić A, Wheeler MF and Wick T. Phase-field modeling of a fluid-driven fracture in a poroelastic medium. *Comput. Geosci.* 2015; 19: 1171-1195.
- Mikelić A, Wheeler MF and Wick T. Phase-field through iterative splitting of hydraulic fractures in a poroelastic medium. Under revision in *GEM Int. J. Geomath* 2018.
- Rutqvist J, Börgesson L, Chijimatsu M, Kobayashi A, Jing L, Nguyen TS, Noorishad J and Tsang CF. Thermohydromechanics of partially saturated geological media: governing equations and formulation of four finite element models. *Int J Rock Mech Min Sci* 2001; 38: 105–127.
- Showalter RE. Diffusion in poro-elastic media. *J. Math. Anal. Appl.* 2000; 251: 310–340.
- Tolstoy, I., *Acoustics, elasticity, and thermodynamics of porous media. Twenty-one papers by M.A. Biot*. New York: Acoustical Society of America, 1992.
- Wick T. Modified Newton methods for solving fully monolithic phase-field quasi-static brittle fracture propagation. *Comp. Meth. Appl. Mech. Engrg.* 2017; 325: 577– 611.